Inorganic Chemistry

Article

pubs.acs.org/IC

Pseudo-symmetry Analysis of the d-block Molecular Orbitals in Four-Coordinate Complexes

Andrés Falceto,[†,§] David Casanova,[‡,§] Pere Alemany,[‡,§] and Santiago Alvarez*[,†,§]

[†]Departament de Química Inorgànica, [‡]Departament de Química Física and [§]Institut de Química Teòrica i Computacional (IQTCUB), Universitat de Barcelona, Martí i Franquès 1-11, 08028 Barcelona, Spain

Supporting Information

ABSTRACT: A rigorous definition of the concept of pseudo-symmetry, which is as important to chemistry as the concepts of symmetry implemented through group theory, should allow us to apply those group theoretical tools to molecules that are significantly distorted from those ideal symmetries best known and understood by the chemical community. In this paper, we consider four-coordinate transition-metal complexes with geometries along the interconversion path between the square and the tetrahedron and show how their molecular orbitals can be expressed in terms of either the tetrahedral or tetragonal symmetry groups. Furthermore, we analyze how the intensity of a d−d absorption band can be related to the degree of symmetry loss of the d-block molecular orbitals by means of their decomposition in terms of contributions from different pseudo-symmetry representations. As a final example, we also show how the substitution of a single ligand in a square planar complex affects the symmetry of the molecular orbitals and the absorption intensity associated to an electronic transition.

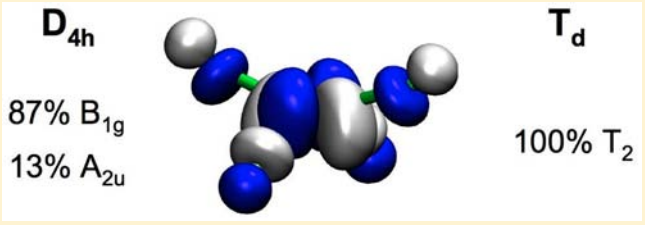

INTRODUCTION

The concept of pseudo-symmetry is embedded in the language of molecular chemistry, even if it is rarely defined. Thus, it is common to consider molecules as if they had a higher symmetry than they actually have, and to talk about *octahedral* complexes, even in cases in which the symmetry around a central metal atom is far from corresponding to the octahedral O_h point group. In general, we can distinguish between such an ideal symmetry group, G, that we should call a *pseudo-symmetry group*, and the actual symmetry group, F, of the molecule under study. For instance, to refer to the d-block molecular orbitals of four-coordinate metal complexes, we often use the e and t_2 symmetry labels valid for the tetrahedral group, even when the molecule under study may be distorted, and we qualify it appropriately as pseudo-tetrahedral.

The use of pseudo-symmetry is useful to keep a consistent conceptual framework and a common language when dealing with several molecules that may belong to different symmetry groups (F_1, F_2, ..., F_n) derived from the same pseudo-symmetry group G (for instance, through different molecular distortions; see Scheme 1). Conversely, one may wish to relate the real symmetry F of a molecule to different ideal symmetries (G_1, G_2, ..., G_n), e.g., looking for patterns of tetrahedral and tetragonal symmetries in four-coordinate metal atoms (see Scheme 2).

However, as powerful as the group theoretical tools are, we have to choose between applying the ideal symmetry in a non rigorous way or to strictly use the real symmetry losing the information associated with the ideal symmetry group, except for the qualitative correlation between irreducible representations of the two groups. Yet, in many applications, it would be highly desirable to be able to apply the group theoretical tools considering the ideal symmetry for a wider perspective, while at the same time using the real one for each particular case. In this work, we apply recent methodological developments in the framework of the continuous symmetry measures (CSMs)[1,2] that allow us to rigorously explore and quantify the symmetry

Scheme 1

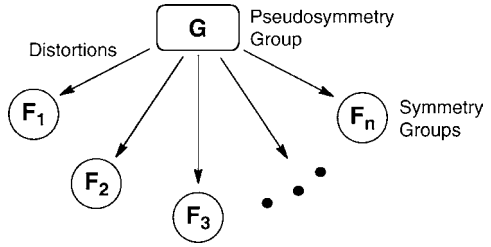

Scheme 2

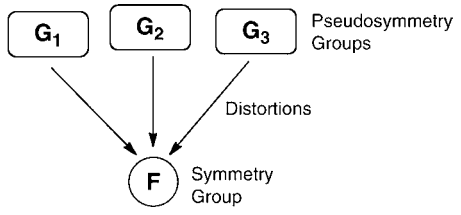

Received: February 22, 2013
Published: May 13, 2013

   dx.doi.org/10.1021/ic4004774 | *Inorg. Chem.* 2013, 52, 6510−6519

of the molecular electronic structure using a pseudo-symmetry point group, and to classify molecular orbitals in terms of its irreducible representations.[3,4] The general problem to which we wish to apply, in a quantitative way, the concepts of pseudo-symmetry is the classification of the molecular orbitals of a molecule belonging to a symmetry group F, according to the irreducible representations of another group G.

In the present work, we show how the use of pseudo-symmetry irreducible representations can be applied to facilitate the analysis of the molecular orbitals (MOs) of four-coordinate complexes. The aspects to be considered are (a) the change in the inversion symmetry properties of the d-block MOs in the frequently found geometries along the D_{2d} spread interconversion pathway (Scheme 3) between the square and the tetrahedron,[5,6] (b) the use of pseudo-symmetry representations to analyze orbital mixing upon distortion along the same pathway, (c) the corresponding pseudo-symmetry analysis of variations in an electronic transition probability upon loss of inversion symmetry along the same path, and (d) the effect of chemical substitution in a square planar complex on the symmetry of its d-block MOs.

Scheme 3

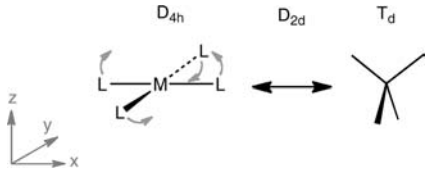

Although the methodology employed here can be applied to molecules of any size, insofar as their MOs can be calculated, we have considered only some of the simplest possible coordination complexes to facilitate a detailed discussion of the details, even at the price of choosing some models that do not have an experimental counterpart. Thus, for the analysis of the inversion properties of d-block MOs, we have chosen the high-spin $[MnF_4]^{2-}$ anion, in which the monatomic ligands avoid symmetry loses due to the presence of substituents, while the high-spin d^5 configuration of the central ion guarantees the same occupation for all the d-orbitals. For the analysis of the orbital mixing on distorting along the spread pathway and the corresponding pseudo-symmetry study of an electronic transition probability, we have chosen the $[NiF_4]^{2-}$ anion for which a z-polarized transition may be ascribed to a single electron excitation from the z^2 to the $x^2 - y^2$ orbital in a hypothetical approximately planar geometry. Finally, to analyze the loss of symmetry of the d-block molecular orbitals of a square planar complex effected by ligand substitution, we have chosen the series of complexes $[Ni^{II}L(PH_3)_3]^{n+}$, where L = PH_3, F^-, Cl^-, Br^-, CN^-, Me^-, and NH_3.

Despite the simplicity of the molecules to be studied here and the relatively high symmetry of the extreme and intermediate structures along the path, the symmetry and composition of the MOs are relatively complicated, as can be seen by analyzing the irreducible symmetry representations of the metal atomic orbitals, with respect to the three point groups that appear along the path, together with those of the symmetry-adapted group orbitals of the ligands (both σ and π), given in Table 1, where the parallel and perpendicular symbols refer to the plane along which the particular ligand is displaced (see Scheme 4 for notation). One can see there that

Table 1. Irreducible Representations of the Metal Atomic Orbitals and of the σ and π-Type Ligand Group Orbitals in a Four-Coordinate Complex along the Spread Pathway from the Square to the Tetrahedron (D_{4h}, D_{2d}, and T_d Point Groups), and upon Substitution of One Ligand in a Square Planar Environment (C_{2v} Point Group)

orbital	D_{4h}	D_{2d}	T_d	C_{2v}
Metal				
z^2	A_{1g}	A_1	E	A_1
xy	B_{2g}	B_1	E	B_1
xz, yz	E_g	E	T_2	$A_2 + B_2$
$x^2 - y^2$	B_{1g}	B_2	T_2	A_1
s	A_{1g}	A_1	A_1	A_1
p_z	A_{2u}	B_2	T_2	B_2
p_x, p_y	E_u	E	T_2	$A_1 + B_1$
Ligand σ				
$\sigma_1 + \sigma_2 + \sigma_3 + \sigma_4$	A_{1g}	A_1	A_1	A_1
$\sigma_1 - \sigma_3$	E_u	E	T_2	A_1
$\sigma_2 - \sigma_4$	E_u	E	T_2	B_1
$\sigma_1 - \sigma_2 + \sigma_3 - \sigma_4$	B_{1g}	B_2	T_2	A_1
Ligand π^a				
$\pi_{1//} - \pi_{2//} + \pi_{3//} - \pi_{4//}$	B_{2u}	A_1	E	B_2
$\pi_{1\perp} - \pi_{2\perp} + \pi_{3\perp} - \pi_{4\perp}$	B_{2g}	B_1	E	B_1
$\pi_{1\perp} + \pi_{2\perp} + \pi_{3\perp} + \pi_{4\perp}$	A_{2g}	A_2	T_1	B_1
$\pi_{1\perp} - \pi_{3\perp}$, $\pi_{2\perp} - \pi_{4\perp}$	E_u	E	T_1	$A_1 + B_1$
$\pi_{1//} + \pi_{2//} + \pi_{3//} + \pi_{4//}$	A_{2u}	B_2	T_2	B_2
$\pi_{1//} + \pi_{3//}$, $\pi_{2//} + \pi_{4//}$	E_g	E	T_2	$A_2 + B_2$

[a]Note: The classification of the π orbitals in two subsets ($\perp$ and //) is not strict for the T_d and D_{2d} symmetries, since each of these subsets by itself is not invariant under the operations of those groups.

Scheme 4

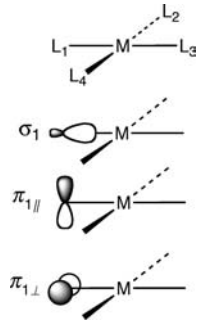

the metal d orbitals can be hybridized in some cases by mixing with metal s or p orbitals of the same symmetry species while they can also interact with ligand orbitals of σ or π type, or both. Let us consider, for example, the z^2 orbital with the help of Table 1. At the square planar geometry (A_{1g} representation), it hybridizes with the s AO and interacts only with ligand σ orbitals (see Figure 1, left). At intermediate geometries along the D_{2d} spread path (A_1 representation), it can mix with both σ and $\pi_{//}$ ligand orbitals (Figure 1, center), whereas at the end of the path, in the tetrahedral geometry (E representation), it can only mix with ligand π orbitals (see Figure 1, right). The types of mixing that z^2 and other d orbitals can present for each symmetry along the path are summarized in Table 2.

The symmetry-controlled changes in the hybridization and in the type of antibonding interaction with ligand orbitals along the path are nicely reflected in the Walsh diagram presented in Figure 2. There, and throughout this paper, we define the geometry of a molecule along the square planar-tetrahedral

dx.doi.org/10.1021/ic4004774 | Inorg. Chem. 2013, 52, 6510−6519

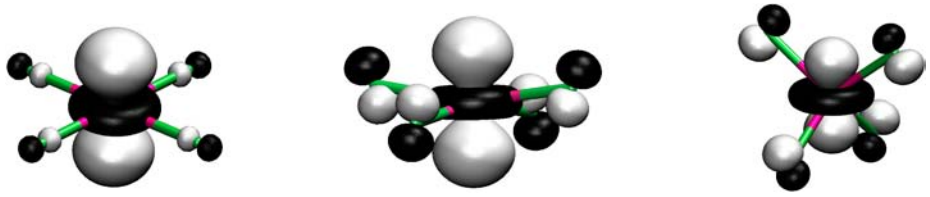

Figure 1. Hybridization of the z^2-type orbital and mixing with different ligand orbitals in the square planar (left), tetrahedral (right) and intermediate (center, 20% along the path to the tetrahedron) geometries of the $[MnF_4]^{2-}$ anion.

Table 2. Symmetry-Allowed Mixing of the d orbitals with Metal s and p Orbitals, and with Ligand σ or π Group Orbitals in an $[MX_4]$ Complex along the Spread Pathway for the Conversion of a Square Planar to a Tetrahedral Coordination Sphere, According to the Irreducible Representations of the Three Relevant Symmetry Groups (Recall Scheme 3)

d orbital	D_{4h}	D_{2d}	T_d
z^2	A_{1g}: s, σ	A_1: s, σ, π	E: π
xy	B_{2g}: π	B_1: π	E: π
xz, yz	E_g: π	E: p_x, p_y, σ, π	T_2: p_x, p_y; σ, π
$x^2 - y^2$	B_{1g}: σ	B_2: p_z, σ, π	T_2: p_z, σ, π

pathway by means of the generalized coordinate[7] along the minimal distortion interconversion pathway,[17] which indicates the portion of the path that a particular structure has covered, from the square (0%) to the tetrahedron (100%). Let us first note that the Walsh diagram predicts the tetrahedral geometry to be the most stable one for a four coordinated d^5 ion such as high-spin Mn^{II}.[8] It is important to notice that, in the square planar geometry, there are four d orbitals that cannot, by the dictate of symmetry rules, mix with the metal s or p orbitals, but they do present σ or π interactions with the ligands in well-known ways (Figure 2, left, upper three orbitals). Only the z^2 orbital can mix with the metal s orbital in such a way as to minimize the antibonding interaction in the xy plane (Figure 2, lowest left orbital). It is thus clear that, along the path, the degree of hybridization and the mixing in of ligand orbitals varies in straightforward ways summarized in Table 2.

At the tetrahedral extreme of the pathway, the three t_2 orbitals of the d-block belong to the same irreducible representation as the valence metal p orbitals, and their mixing results in hybridization of the occupied orbitals in such a way as to minimize the antibonding interaction with the ligands, as illustrated in Scheme 5. As a result, the d-block molecular

Scheme 5

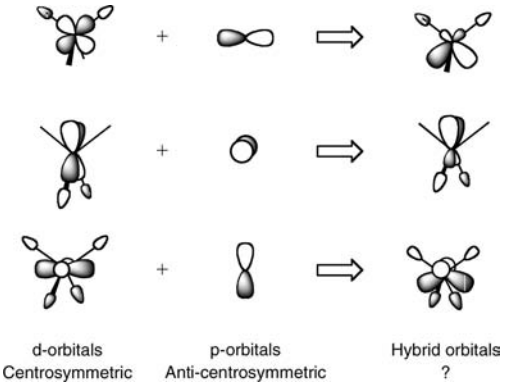

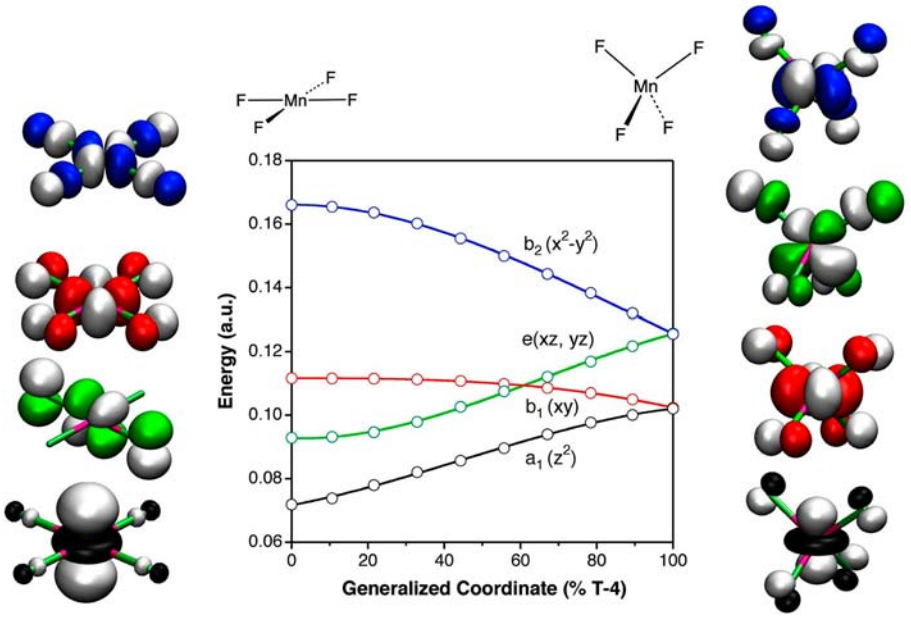

Figure 2. Walsh diagram for the d-block molecular orbitals of the $[MnF_4]^{2-}$ anion along the spread pathway. The energies and compositions of the molecular orbitals obtained through density functional theory (DFT) calculations are drawn as 0.04 probability contours. The symmetry labels given correspond to the D_{2d} point group. For the sake of clarity, only one of the two equivalent orbitals of the (xz, yz) set is shown at each side of the diagram.

dx.doi.org/10.1021/ic4004774 | Inorg. Chem. 2013, 52, 6510−6519

orbitals present a small gap separating the e and t_2 subsets, and the latter should be considered as *formally nonbonding*.[9] That small gap (5100 cm^{-1} in the present calculations) is responsible for the well-known tendency of open shell tetrahedral complexes to present high spin states, as well as for the low energy of their d-d electronic transitions in their visible spectra. Yet another consequence of that mixing is the incorporation of some anticentrosymmetric character into the otherwise centrosymmetric d-block orbitals.

ORBITAL MIXING AND LOSS OF INVERSION SYMMETRY

Since inversion symmetry of the molecular orbitals is of the utmost importance in determining the intensities of the electronic spectral bands, according to the well-known Laporte rule,[10] it is worth exploring how the symmetry measures[3,4] of the d-block MOs of a four-coordinate complex can provide us with a quantitative description of the loss of inversion symmetry associated to the orbital mixing just discussed (Scheme 5). For that purpose, we have calculated the symmetry measures of the d-block MOs of the $[MnF_4]^{2-}$ anion along the spread pathway relative to the C_i symmetry group. Note that, in this case, C_i is only a subgroup of the molecular symmetry group at the beginning of the path, for the square planar structure. All other structures along the path do not have an inversion center, although in the language of continuous symmetry measures the degree of inversion symmetry is considered to diminish continuously as we depart from the initial D_{4h} geometry.

In Figure 3, we compare the inversion group measures[2] $S(C_i)$ for the MnF_4 nuclear framework and those for its five d-block

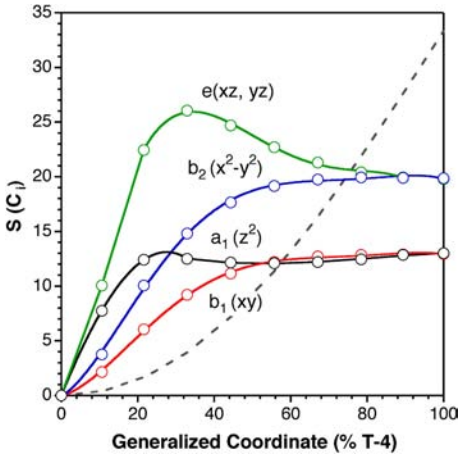

Figure 3. Inversion measures of the d-block MOs of $[MnF_4]^{2-}$ along the spread pathway from square planar (0%) to tetrahedral (100%). The inversion measure for the nuclear framework is represented as a dashed line, for the sake of comparison.

MOs, as a function of the generalized coordinate for the spread path used above for Figure 2. There, we see that the inversion symmetry measure of the nuclear skeleton increases continuously along the square-tetrahedron pathway, as was to be expected. The five d-block MOs have zero values of $S(C_i)$ at the square planar geometry or, in other words, they are all fully g-type orbitals. In contrast with the nuclear framework, however, they lose inversion symmetry at a higher pace for small distortions, but halfway to the tetrahedron, their degrees of asymmetry asymptotically converge to two distinct inversion measure values for the e and t_2 MO sets of the tetrahedron. The loss of inversion symmetry of those MOs is due to the combined effect of mixing in u-type metal p orbitals and the loss of inversion symmetry of the ligand group orbitals that participate in those MOs. Therefore, the limiting values at the tetrahedral geometry are determined by the weight of the centrosymmetric metal d orbitals in those MO sets, and they explain the much less centrosymmetry content (higher C_i measure) of the t_2 orbitals compared to the e ones (see Scheme 5). The behavior of the e(*xz*,*yz*) pair of orbitals at intermediate geometries is, at first glance, surprising, showing a maximum in its loss of g symmetry at about one-third of the pathway, and decreasing again as the tetrahedron is approached. The discussion of this issue will be highly facilitated by analysis of the pseudo-symmetry representations and will be addressed after introducing such an analysis in the next section.

ORBITAL MIXING AND PSEUDO-SYMMETRY REPRESENTATIONS

The question we wish to address in this section is this: Can we adopt a unique symmetry-based notation for the molecular orbitals, avoiding the use of different symmetry labels for the molecular orbitals corresponding to the three different point groups appropriate for the tetrahedral, intermediate, and square planar geometries? To answer that question, we will make use of the pseudo-symmetry measures of irreducible representations.[4,11]

We have recently shown that any molecular orbital ϕ_i in a molecule with symmetry F can be expanded as a pseudo-symmetry-adapted linear combination (PSALC) of orbitals φ_{ij}^{μ} that belong to irreducible representations Γ^{μ} of a pseudo-symmetry group G ≠ F, according to the following expression:[11]

$$\phi_i = \sum_{\mu}^{N_{IR}} \sum_{j}^{d_\mu} c_{ij}^{\mu} \varphi_{ij}^{\mu} \tag{1}$$

where the sum extends over all the N_{IR} irreducible representations of the pseudo-symmetry group G, d_μ is the dimension of the μth IR of G, and $\{c_{ij}^{\mu}\}$ a set of coefficients that calibrate the participation of each representation in ϕ_i.

Such an approach allows us to easily analyze orbital mixing due to symmetry lowering in the intermediate four-coordinate structures along the square planar-tetrahedral pathway, relative to either of the two ideal symmetries. Because of orthonormality of the $\{\varphi_{ij}^{\mu}\}$ set, the weight of each $\{\varphi_{ij}^{\mu}\}$ in ϕ_i is directly obtained as in eq 2a, where we can drop the *j* subindex for nondegenerate representations (eq 2b).

$$\omega_i^{\mu} = \sum_{j}^{d_\mu} |c_{ij}^{\mu}|^2 \tag{2a}$$

$$\omega_i^{\mu} = (c_i^{\mu})^2 \tag{2b}$$

Let us consider only the examples of the x^2-y^2 and z^2-type MOs of the $[NiF_4]^{2-}$ anion, since we will later focus on an electronic transition involving those two orbitals. If we adopt D_{4h} as the pseudo-symmetry group for an arbitrary geometry along the D_{2d} planarization pathway, eq 1 for each of those MOs leads to eqs 3 and 4, where a_{1g}, for instance, represents all the orbital contributions that belong to the A_{1g} representation of the pseudo-symmetry group D_{4h}.

dx.doi.org/10.1021/ic4004774 | Inorg. Chem. 2013, 52, 6510−6519

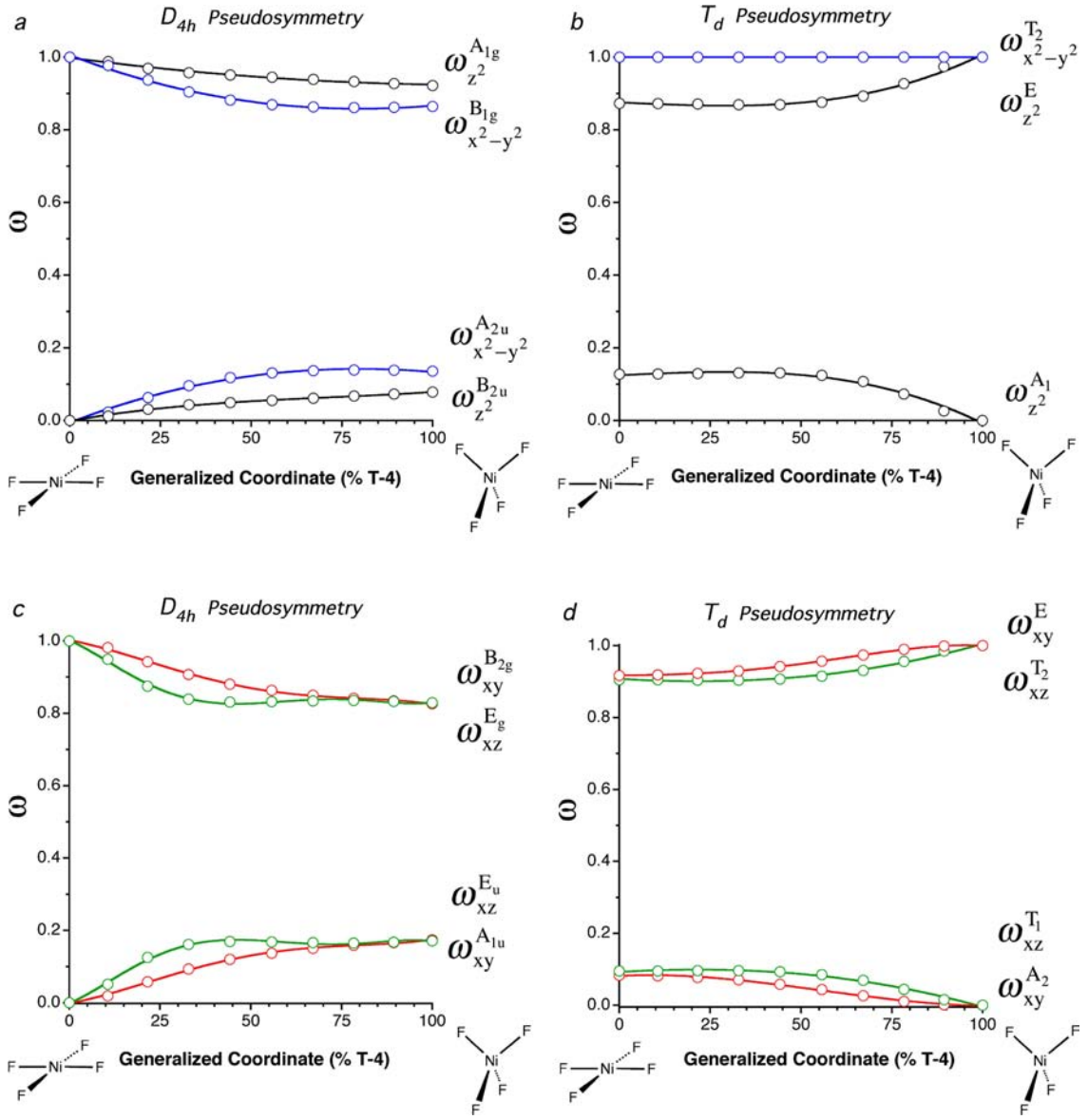

Figure 4. Weights of the pseudo-symmetry representations for the d-based molecular orbitals of the $[NiF_4]^{2-}$ anion along the square to tetrahedron pathway, relative to (a, c) the D_{4h} pseudo-symmetry groups and (b, d) the T_d pseudo-symmetry groups.

$$\phi_{z^2} = c_{z^2}^{A_{1g}} a_{1g} + c_{z^2}^{B_{2u}} b_{2u} \quad (3)$$

$$\phi_{x^2-y^2} = c_{x^2-y^2}^{B_{1g}} b_{1g} + c_{x^2-y^2}^{A_{2u}} a_{2u} \quad (4)$$

In these equations, we see that the mixing of orbitals of different D_{4h} representations upon symmetry descent is quite simple. A look at the symmetry representations of the metal and ligand orbitals in the D_{2d} group (Table 1) helps us in obtaining a deeper insight on such expressions. It can be seen, e.g., that the only orbital of non-A_{1g} pseudo-symmetry that can mix with $a_{1g}(z^2)$ upon symmetry descent to the D_{2d} group is the ligand $b_{2u}(\pi_{//})$ orbital, since both belong to the $A_1(D_{2d})$ representation, hence the simple expression of eq 3. Similarly, the $b_{1g}(x^2 - y^2)$ MO is allowed upon distortion to incorporate only new contributions from the metal p_z atomic orbital and from a ligand π orbital, $a_{2u}(\pi_{//})$, as reflected in eq 4.

Of course, the exact values of the mixing coefficients for a given complex depend on the degree of distortion from the square planar geometry. We illustrate the evolution of the composition of the z^2 and $x^2 - y^2$-based MOs by plotting the weights ω_{MO}^{μ} defined in eqs 2 along the spread pathway (see Figure 4a), where ω_{MO}^{μ} represents the weight of the functions belonging to the pseudo-symmetry representation Γ^{μ} in the given MO (for simplicity, here, we use z^2 and $x^2 - y^2$ to refer to the z^2- and $(x^2 - y^2)$-based MOs). We can do that taking either tetragonal pseudo-symmetry (Figures 4a and 4c) or tetrahedral pseudo-symmetry (Figures 4b and 4d).

As expected, we observe in Figure 4a that the z^2-MO has strict A_{1g} symmetry at the square planar geometry, as indicated by the values $\omega_{z^2}^{A_{1g}} = 1$ and $\omega_{z^2}^{B_{2u}} = 0$. A distortion of 11% toward the tetrahedron is sufficient to incorporate some noticeable B_{2u} character ($\omega_{z^2}^{B_{2u}} = 0.012$), that can only come from mixing with a ligand group orbital of $\pi_{//}$ character (see Table 1). The B_{2u} contribution increases as the distortion progresses, reaching a maximum at the tetrahedral geometry ($\omega_{z^2}^{B_{2u}} = 0.078$), but it is clear that the weight of the A_{1g} contribution remains dominant all the way to the tetrahedron. Therefore, one can reasonably continue to use the a_{1g} pseudo-symmetry label for that MO,

dx.doi.org/10.1021/ic4004774 | Inorg. Chem. 2013, 52, 6510−6519

even at highly distorted geometries along the spread path. Something similar happens with the b_{1g} orbital, even if the mixing in that case is somewhat more important and involves contributions of A_{2u} symmetry that can only come from the metal p_z atomic orbital and from a ligand orbital of $\pi_{//}$ character (Table 1). The actual compositions of those two MOs at an intermediate geometry are shown in Figure 5, where

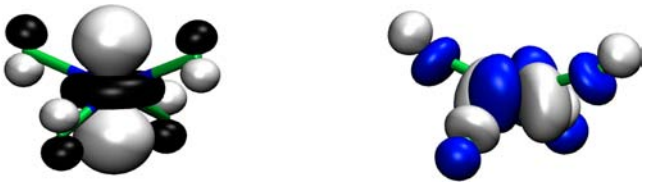

Figure 5. Composition of the z^2- and $(x^2 - y^2)$-type MOs of the $[NiF_4]^{2-}$ anion in an intermediate geometry along the spread pathway, showing the mixing with a ligand $b_{2u}(\pi_{//})$ orbital and the hybridization with the metal $b_{2u}(p_z)$ orbital, respectively (see Scheme 5).

we can see that the inclusion of ligand $\pi_{//}$ contribution (Scheme 4) to $x^2 - y^2$ allows donor orbitals to deviate from the ligand−metal direction in the nonplanar molecule, thus optimizing their overlap with the metal $x^2 - y^2$ orbital.

Alternatively, one could carry out a similar analysis with respect to the tetrahedral pseudo-symmetry (see Figures 4b and 4d). A remarkable feature is that the $(x^2 - y^2)$-based MO retains the full T_2 symmetry throughout the path. This does not mean that there are no changes in its composition, but that those changes (replacement of π-ligand orbitals by σ-ligand orbitals as one moves to the left in the diagram, toward the square) do not imply mixing with orbitals of different representations in the extreme tetrahedral geometry. On the other hand, the z^2-type MO belonging to the E representation at the tetrahedron, rapidly incorporates A_1 character as the molecule is planarized (i.e., on going from right to left in Figure 3a), because of the $s + z^2$ hybridization forbidden in the T_d but allowed in the D_{2d} and D_{4h} groups. Interestingly, that mixing reaches a plateau before the middle of the planarization pathway, remaining constant all the way to the square.

The other d-block MOs behave in a similar way (Figure 4d). In summary, we can say that it is reasonable to use the irreducible representations of either the T_d or the D_{4h} pseudo-symmetry groups to label the d-block MOs along the planar to tetrahedral pathway of a tetracoordinate complex, since their composition has a predominant contribution from the corresponding symmetry species. The analysis presented here allows us to quantify the degree to which such a labeling can be trusted at any particular point of the path and also facilitates enormously the task of identifying which orbitals are mixing into the d-type orbitals upon symmetry descent. It must be stressed that such an analysis is made in an automatic fashion by means of the Wave-Sym program[11] and provides simple results that are hampered by neither the complexity of the basis set used, nor the mixing of different MOs of the same symmetry.

We can go back now to the discussion of the presence of a maximum in the inversion symmetry measure of the e(*xz*,*yz*) pair of orbitals at geometries intermediate between the square and the tetrahedron (Figure 3). The contribution of the E_u (D_{4h} group) representation to each of those degenerate orbitals is found to increase from 0 at the square planar geometry to 23% at the midpoint, and then decrease to 20% at the end of the pathway. Inspection of Table 1 tells us that such behavior should be ascribed to the mixing in of the $e_u(\pi_\perp)$ orbitals, allowed in the D_{2d} group (E representation) but not in the T_d group (T_1 representation), while the remaining E_u contribution in the tetrahedron is due to the $e_u(p_x,p_y)$ and $e_u(\sigma)$ pairs that belong to the same representation as the (*xz*,*yz*) set in both the D_{2d} and T_d symmetry groups (E and T_2, respectively).

PSEUDO-SYMMETRY ANALYSIS OF ELECTRONIC TRANSITION PROBABILITIES

The presence or absence of inversion symmetry has a strong influence on the intensity of the electronic absorption bands, according to the Laporte rule.[10] That rule is just a simplification, albeit a useful one, of the more general symmetry selection rules that requires the direct product of the irreducible representations of the ground and excited states to contain the representation of a component of the dipole moment. By focusing only on the inversion operation, one can conclude that the only nonvanishing electric-dipole transition moments are those that connect an even (g) and an odd (u) term. Hence, the "d → d" transitions are forbidden by symmetry in square planar and octahedral complexes, and such transitions are seen in visible spectra only as relatively weak bands, thanks to vibronic coupling that renders the Laporte rule only approximate. However, along the distortion path from the square to the tetrahedron, the mixing of g and u orbitals just discussed (Scheme 5) results in a nonstrict applicability of the Laporte rule and significantly enhanced intensities of the d → d absorption bands.

We can go now a step further and analyze the variation of the intensities of the d → d transitions along the spread pathway by means of the pseudo-symmetry properties of the d-block orbitals. To that end, we focus on the $^1A_{1g} \rightarrow {}^1B_{1g}$ transition (D_{4h} pseudo-symmetry labels) of the d^8 $[NiF_4]^{2-}$ anion, that corresponds essentially to a $z^2 \rightarrow x^2 - y^2$ one-electron excitation. For that purpose, we performed TD-DFT (see the Methods section) calculations for that anion at several geometries along the minimal distortion interconversion pathway, from which we obtained the calculated intensity for that transition at each geometry between the square planar and tetrahedral extremes. The reader must be reminded that at the tetrahedral extreme of the pathway the singlet state is no longer the ground state, although we carry out our analysis for the full path in order to provide a broader picture.

The intensity of the absorption band associated to an electronic transition between the ground and excited states Ψ_0 and Ψ_n is proportional to the oscillator strength f_{0n} (eq 5):[12]

$$f_{0n} = \frac{2\Delta E_{0n}}{3h^2}\left|\left\langle \Psi_0 \middle| \vec{\mu} \middle| \Psi_n \right\rangle\right|^2 \tag{5}$$

where $\left\langle \Psi_0 \middle| \vec{\mu} \middle| \Psi_n \right\rangle$ is the transition dipole moment integral, ΔE_{0n} is the energy difference between the two states, and $\vec{\mu}$ is the dipole moment operator. For one-electron transitions that involve only an occupied orbital *i* and an empty orbital *a*, the transition dipole moment integrals can be approximated in terms of the molecular orbitals:

$$\left\langle \Psi_0 \middle| \vec{\mu} \middle| \Psi_n \right\rangle \approx \left\langle \phi_i \middle| \vec{\mu} \middle| \phi_a \right\rangle \tag{6}$$

For the particular one-electron excitation from z^2 to $x^2 - y^2$, the introduction of the D_{4h} pseudo-symmetry expression of the

dx.doi.org/10.1021/ic4004774 | Inorg. Chem. 2013, 52, 6510−6519

wave functions for the ground and excited states (eqs 3 and 4) yields

$$\langle \phi_i|\mu_z|\phi_a\rangle = c^{B_{1g}}_{x^2-y^2} c^{A_{1g}}_{x^2} a_{1g}\langle b_{1g}|\mu_z|a_{1g}\rangle + c^{B_{1g}}_{x^2-y^2} c^{B_{2u}}_{z^2}\langle b_{1g}|\mu_z|b_{2u}\rangle + c^{A_{2u}}_{x^2-y^2} c^{A_{1g}}_{z^2} a_{1g}\langle a_{2u}|\mu_z|a_{1g}\rangle + c^{A_{2u}}_{x^2-y^2} c^{B_{2u}}_{z^2}\langle a_{2u}|\mu_z|b_{2u}\rangle \quad (7)$$

Given the anticentrosymmetric character of the components of the dipole moment, belonging to the A_{2u}(z-component) and E_u (x- and y-components) representations of the D_{4h} group, the first and last terms of eq 7 are rigorously zero, and so are the contributions from the x- and y-components of $\vec{\mu}$. Consequently, we are left with the following expression for the probability integral:

$$\langle \phi_i|\mu_z|\phi_a\rangle = c^{B_{1g}}_{x^2-y^2} c^{B_{2u}}_{z^2}\langle b_{1g}|\mu_z|b_{2u}\rangle + c^{A_{2u}}_{x^2-y^2} c^{A_{1g}}_{z^2}\langle a_{2u}|\mu_z|a_{1g}\rangle \quad (8)$$

To get a rough idea of how that integral evolves along the spread pathway, we assume as a crude approximation that the two integrals at the right-hand side of eq 8 have similar values,

$$\langle b_{1g}|\mu_z|b_{2u}\rangle \approx \langle a_{2u}|\mu_z|a_{1g}\rangle = k$$

then deduce a further simplified expression for the transition dipole integral as a function of a sum of products of pseudo-symmetry coefficients,

$$\langle \phi_i|\mu_z|\phi_a\rangle \approx k\left(c^{B_{1g}}_{x^2-y^2} c^{B_{2u}}_{z^2} + c^{A_{2u}}_{x^2-y^2} c^{A_{1g}}_{z^2}\right) \quad (9)$$

and obtain the following approximate expression for the oscillator strength (eq 5):

$$\frac{f_{0n}}{\Delta E_{0n}} \approx \kappa\left(c^{B_{1g}}_{x^2-y^2} c^{B_{2u}}_{z^2} + c^{A_{2u}}_{x^2-y^2} c^{A_{1g}}_{z^2}\right)^2 \quad (10)$$

where κ is a constant.

Therefore, the symmetry-allowedness of the $z^2 \rightarrow x^2 - y^2$ transition in a square planar complex distorted along the spread pathway depends crucially on the mixing coefficients $c^{B_{2u}}_{z^2}$ and $c^{A_{2u}}_{x^2-y^2}$. Again, a look at Tables 1 and 2 allows us to conclude that those coefficients reflect the mixing of a ligand π orbital of B_{2u} symmetry with z^2, and of $x^2 - y^2$ with the metal p_z and a ligand π orbital, both of A_{2u} symmetry.

In the specific case of $[NiF_4]^{2-}$, that excitation is strictly symmetry-forbidden in the square planar geometry but partially symmetry-allowed in the tetrahedral conformation, and its calculated oscillator strength behaves as expected, with a monotonous increase along the spread pathway (Figure 6). Given the dependence of the mixing coefficients on the generalized coordinate discussed above, we also expect the symmetry product (right-hand side of eq 10) to increase along the path, as actually seen in Figure 6, indicating an almost-parallel behavior of the oscillator strength and the symmetry product, which is reflected in a fair nonlinear correlation between the two parameters. The differences between the two curves should without doubt be attributed to the crude approximation made in deducing eqs 9 and 10 concerning the two integrals that appear in eq 8. Despite such a crude approximation, the product of coefficients nicely predicts the qualitative behavior of the intensity of the $z^2 \rightarrow x^2 - y^2$ band along the pathway, indicating that the changes in those coefficients, i.e., the mixing of orbitals brought about by symmetry descent, are perhaps more important than the variation of the transition integrals.

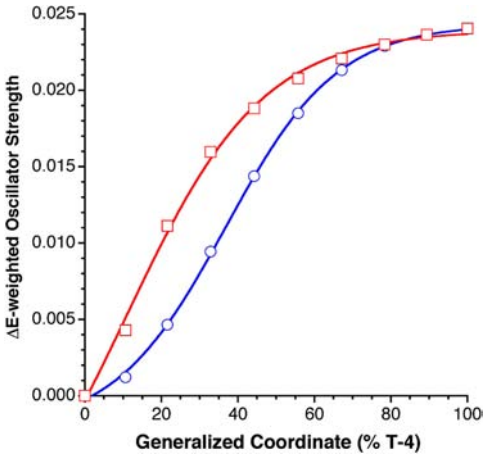

Figure 6. Calculated ΔE−weighted oscillator strength for the $z^2 \rightarrow x^2 - y^2$ transition in $[NiF_4]^{2-}$ along the spread pathway from the square to the tetrahedron (circles), compared to the variation of the pseudo-symmetry coefficients (fitted to eq 10 with $\kappa = 0.064$) along the same path (squares).

The symmetry allowedness of the $z^2 \rightarrow x^2 - y^2$ transition, neglecting vibronic coupling, increases gradually from strictly forbidden at the square planar geometry to an asymptotic maximum at geometries with ∼60% tetrahedral character. Therefore, these results rationalize, in an elegant way, the well-known difference in the intensity of the d → d bands in visible spectra of square planar and tetrahedral complexes.[13] It is appropriate to recall here that it has been previously shown how the position of the lowest energy absorption band in some four-coordinate Cu^{II} complexes can be correlated to the degree of tetrahedricity of the Cu coordination sphere.[14] Other spectroscopic probes along that pathway have also been analyzed by Solomon.[15]

EFFECTS OF CHEMICAL SUBSTITUTION ON ORBITAL PSEUDO-SYMMETRY

In the previous sections, we have analyzed the symmetry changes that accompany a geometric distortion for the same metal ion and coordination sphere, as well as their effect on the composition of the d-block molecular orbitals and the symmetry allowedness of electronic transitions. Now we take a different point of view, starting from a square planar coordination sphere and inducing symmetry changes in the electronic structure only by means of a ligand substitution, without altering the basic square planar geometry of the coordination sphere. We take, as our workhorse, a group of $[Ni^{II}(PH_3)_3X]^{n+}$ complexes, with X = PH_3, F^-, Cl^-, Br^-, CN^-, NH_3, and CH_3^-.

The symmetry lowering from D_{4h} to C_{2v} upon substitution of one phosphine in $[Ni(PH_3)_4]^{2+}$ by a halide results in mixing of the empty ($x^2 - y^2$)-type MO with occupied orbitals, with a resulting significant localization of three orbitals of A_1 symmetry (see Figure 7): While the empty $3a_1$ becomes essentially $x^2 - y^2$ with σ^* Ni−X character, the occupied orbitals $1a_1$ and $2a_1$ become essentially Ni−P and Ni−X σ bonding, respectively. How that mixing occurs can be deduced effortlessly by the pseudo-symmetry representation decomposition of that MO (see Table 3), which is visually summarized in Scheme 6, where the mixing coefficients for a given complex are related to the weights given in Table 3 through eq 2b.

dx.doi.org/10.1021/ic4004774 | Inorg. Chem. 2013, 52, 6510−6519

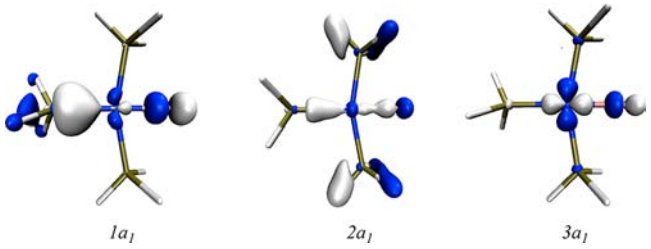

Figure 7. Localization of the empty $3a_1(x^2 - y^2)$ MO and other occupied orbitals of the same symmetry in $[NiF(PH_3)_3]^+$, as a result of symmetry lowering from D_{4h} to C_{2v}.

Table 3. Orbital Contributions to the $(x^2 - y^2)$-Type MO ($3a_1$) of the $[Ni^{II}X(PH_3)_3]^{n+}$ Complexes (X = PH_3, Br, Cl, and F), in Terms of the Irreducible Representations of the Pseudo-symmetry D_{4h} Point Group

	Orbital Contributions (%)			
X	$\omega_{3a_1}^{B_{1g}}$	$\omega_{3a_1}^{E_u}$	$\omega_{3a_1}^{A_{1g}}$	other
PH_3	97.3	0.7	0.0	2.0
Br	94.5	3.5	1.0	1.0
Cl	92.8	5.2	1.8	0.2
F	80.8	13.0	5.9	0.3

Note that the optimized geometries indicate a decreasing X–Ni–P_{cis} bond angle as the E_u contribution to $3a_1(x^2 - y^2)$ increases (i.e., from PH_3 to Br to Cl to F; see Table 4), which could be interpreted as an increasing tendency to employ mostly the $x^2 - y^2$ orbital for bonding to X and a preferential sp^2 bonding with the phosphines. This interpretation can be verified in Table 4, where we see that the $3a_1(x^2 - y^2)$ empty MO has an increasing metal d contribution along the series. The closing of the X–Ni–P_{cis} bond angle as the phosphine group is substituted by bromide, chloride, and fluoride could, in principle, be described as a tendency toward a partial dissociation to a trigonal planar $[Ni(PH_3)_3]^{2+}$ molecule linked via ionic interaction with a halide (see Scheme 7). This qualitative description of the observed distortion finds a quantitative expression if we plot the percentage of the dissociation path defined by shape measures[16] of the $Ni(PH_3)_3$ fragment as a function of the electronegativity of the donor atom (see Figure 8). Moreover, a nice correlation has been found between the electronegativity of the donor atom X and its calculated atomic charge, which is consistent with the increasing ionic character of the Ni–X bond along the series.

We now wish to examine the effect of the symmetry lowering in the series of $[Ni^{II}(PH_3)_3X]^{n+}$ complexes, brought about by chemical substitution, on the intensity of the absorption band associated to the $z^2 \rightarrow x^2 - y^2$ electronic transition. It must be mentioned that the two bonding isomers $[Ni(PH_3)_3NCS]^+$ and $[Ni(PH_3)_3SCN]^+$ have been disregarded for this study, since that electronic transition cannot be reasonably ascribed to single MOs, because of extensive mixing of the z^2 orbital with the π-system of the thiocyanato ligand that introduces significant charge-transfer character to that transition. The symmetry descent to the C_{2v} point group produced by chemical substitution also allows mixing of the $x^2 - y^2$ and z^2 orbitals (both belonging to the A_1 representation in C_{2v}) with each other, as well as with orbitals of the E_u representation of the D_{4h} pseudo-symmetry group (see Table 1 for compositions of the orbitals of those symmetries). Since the incorporation of anticentrosymmetric E_u contributions is expected to make the $z^2 \rightarrow x^2 - y^2$ transition partially symmetry-allowed, we have analyzed the weights of the E_u contributions to those two MOs. We can deduce an expression similar to eq 8 that relates the oscillator strength to the weights of the different pseudo-symmetry representations, including four terms in this case:

$$\langle \phi_i | \mu_{x,y} | \phi_a \rangle = c_{z^2}^{A_{1g}} c_{x^2-y^2}^{E_u} \langle a_{1g} | \mu_{x,y} | e_u' \rangle + c_{z^2}^{B_{1g}} c_{x^2-y^2}^{E_u} \langle b_{1g} | \mu_{x,y} | e_u' \rangle + c_{z^2}^{E_u} c_{x^2-y^2}^{A_{1g}} \langle e_u | \mu_{x,y} | a_{1g}' \rangle + c_{z^2}^{E_u} c_{x^2-y^2}^{B_{1g}} \langle e_u | \mu_{x,y} | b_{1g}' \rangle \quad (11)$$

Of all the products of coefficients that appear in eq 11, the first and last ones are sufficiently large to make the corresponding terms non-negligible. As a consequence, the oscillator strength cannot be correlated to a single parameter, except for the series of halo-substituted complexes, for which the first term predominates (see the Supporting Information). In that case, a nice correlation is seen between the degree of mixing of orbitals of $E_u(D_{4h})$ character into the $(x^2 - y^2)$-type MO and the calculated oscillator strength. The different nature of the other ligands considered results in nonsystematic variations of the values of the pseudo-symmetry coefficients and probably also of the corresponding integrals. For the halo-substituted complexes, inspection of the weights of the different pseudo-symmetry representations in the z^2- and $(x^2 - y^2)$-based MOs shows that the former incorporates very little E_u character, whereas $3a_1(x^2 - y^2)$ strongly mixes with the halide

Scheme 6

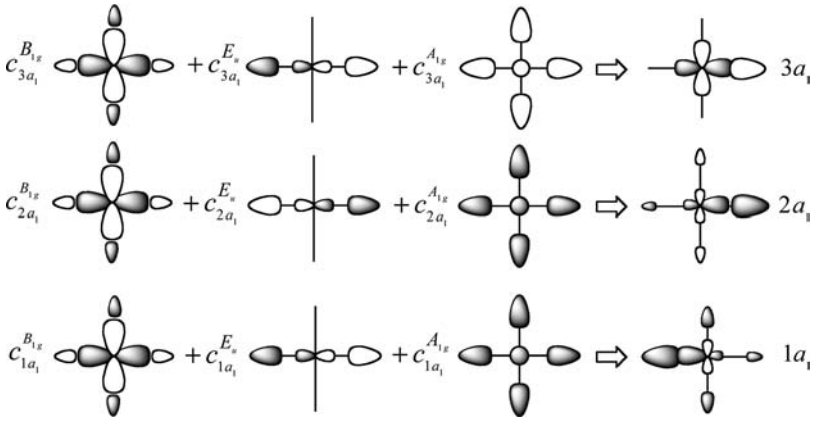

dx.doi.org/10.1021/ic4004774 | Inorg. Chem. 2013, 52, 6510–6519

Table 4. Calculated Ni–X Bond Distances, P_{cis}–Ni–P_{cis} Bond Angles, and Orbital and Atomic Contributions to the $(x^2 - y^2)$-Type MO of the $[Ni^{II}X(PH_3)_3]^{n+}$ Complexes (X = PH_3, Br, Cl, and F)

			Contributions (%)						
X	bond distance, Ni–X (Å)	bond angle, α (deg)	Ni (d)	Ni (s)	Ni (p)	X	P_{trans}	P_{cis}	
PH_3	2.263	180.0	43.0	0.0	0.0	10.7	10.7	10.3	10.0
Br	2.323	168.0	44.0	0.1	0.1	15.3	9.0	10.2	10.0
Cl	2.174	166.7	45.0	0.2	0.1	13.0	9.0	9.7	9.4
F	1.792	160.4	49.4	0.2	0.5	8.9	8.3	10.7	10.7

Scheme 7

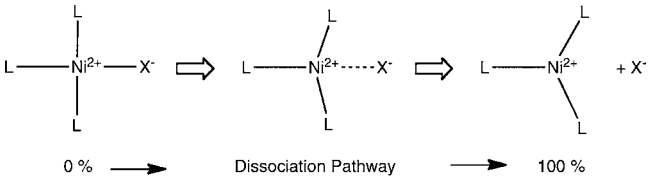

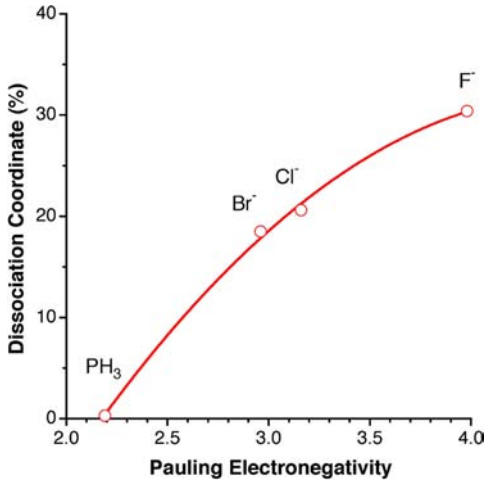

Figure 8. Position of the $NiX(PH_3)_3$ fragment of the $[Ni^{II}X(PH_3)_3]^{n+}$ complexes (X = PH_3, Br^-, Cl^-, and F^-) along the dissociation path of Scheme 7 (shown as a percentage), as a function of the Pauling electronegativity of X.

σ-lone pair (Figure 7), thus introducing significant E_u contributions, which are responsible for the dominant character of $\omega^{E_u}_{x^2-y^2}$ in the value of the oscillator strength. Therefore, within this series of complexes, the oscillator strength is well-correlated with the value of that parameter, as seen in Figure 9a.

In addition, in the series of halo-substituted complexes, it is seen that the E_u contribution to the $(x^2 - y^2)$-based MO is well-correlated to the electronegativity of the halide. As a consequence, the oscillator strength is also correlated to the electronegativity of the halide. A plot of the band intensity as a function of the relative electronegativity of the donor atom substituted for a phosphine shows a clear dependence of the oscillator strength on the relative electronegativity of the donor atom when similar ligands are considered (PH_3, CH_3^-, and NH_3, or F^-, Cl^-, and Br^-; see Figure 9b). Remarkably, the π-acceptor cyanide ligand seems to follow the same electronegativity dependence than the π-donor halo ligands, thus confirming that the main effect is the incorporation of E_u character into the $(x^2 - y^2)$-type MO via σ-antibonding interaction with the heteroligand X.

CONCLUSIONS

As the first examples of the pseudo-symmetry decomposition of molecular orbitals are presented in this paper, we have carried out a detailed group theoretical analysis of the orbital correlations along the square planar to tetrahedral pathway for four-coordinate complexes, to verify that the results follow the qualitative expectations. However, one can from now on employ the pseudo-symmetry decomposition in an automatic way without the need of an a priori group theoretical analysis.

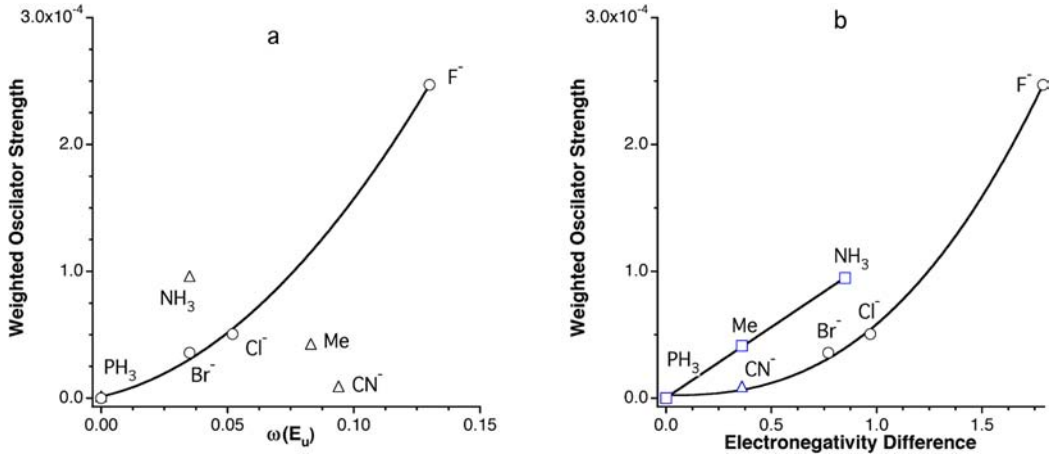

Figure 9. Calculated oscillator strength weighted by the energy gap as a function of (a) the weight of the E_u contribution to the $(x^2 - y^2)$-type molecular orbital in $[Ni^{II}(PH_3)_3X]^{n+}$ (X = PH_3, Br^-, Cl^-, and F^-, denoted by circles (○); other ligands are represented by triangles (△)), and (b) of the difference in electronegativity of the donor atoms in the series of complexes $[Ni^{II}(PH_3)_3X]^{n+}$ (X = PH_3, Br^-, Cl^-, and F^-, denoted by circles) and $[Ni^{II}(PH_3)_3(YH_3)]^{n+}$ (Y = P, C, and N, denoted by squares).

dx.doi.org/10.1021/ic4004774 | Inorg. Chem. 2013, 52, 6510–6519

In the particular case of the four-coordinate transition-metal complexes, we have shown that the d-block MOs for geometries intermediate between square planar and tetrahedral can, to a very good approximation, be referred using the pseudo-symmetry labels of either of the two ideal geometries at the extremes of that pathway. If need be, one can also obtain a quantitative description of the mixing of orbitals of different pseudo-symmetry species. For the case of the $z^2 \rightarrow x^2 - y^2$ electronic transition in Ni^{II} complexes, we have shown that the intensity of the corresponding absorption band can be roughly correlated to the weights of anticentrosymmetric metal or ligand orbitals mixed into the z^2- and $(x^2 - y^2)$-based MOs. It has also been shown how chemical substitution in a square planar complex introduces a loss of symmetry in the d-block MOs.

METHODS

Structures along the minimal distortion pathway between the square and the tetrahedron,[17] which is usually referred to as the spread pathway, have been obtained with the SHAPE program.[18] The alternative twist pathway is adequate only when bidentate ligands are involved,[19] and that has not been considered in the present work.

All calculations have been done with the B3LYP functional[20] and the Def2-TZVP basis set.[21] Structures along the spread pathway of $[MnF_4]^{2-}$ and $[NiF_4]^{2-}$ ions have been constructed fixing the Mn−F and Ni−F distances optimized for the T_d geometry. Electronic transitions for the $[NiF_4]^{2-}$ and $[Ni(PH_3)_3X]^{n+}$ compounds have been obtained within the TD-DFT methodology at the B3LYP/Def2-TZVP level.

Electronic wave functions have been obtained with the Q-Chem package,[22] while the symmetry decomposition analysis of the molecular orbitals was performed with a development version of the Wave-Sym program[11] written by the authors.

ASSOCIATED CONTENT

Supporting Information

This material is available free of charge via the Internet at http://pubs.acs.org.

AUTHOR INFORMATION

Corresponding Author

*Tel.: 34 93-402-1269. Fax: 34 93-490-7725. E-mail: santiago.alvarez@qi.ub.es.

Notes

The authors declare no competing financial interest.

ACKNOWLEDGMENTS

This work was supported by the Spanish Ministerio de Economía y Competitividad (Project Nos. CTQ2011-23862-C02-01 and CTQ2011-23862-C02-02) and by the Generalitat de Catalunya (Project No. 2009SGR-1459). D.C. gratefully acknowledges the Ramón y Cajal Program (No. RyC 2008-0223) for financial support.

REFERENCES

(1) (a) Zabrodsky, H.; Peleg, S.; Avnir, D. *J. Am. Chem. Soc.* **1992**, *114*, 7843. (b) Casanova, D.; Alemany, P.; Alvarez, S. *J. Comput. Chem.* **2010**, *31*, 2389. (c) Pinsky, M.; Dryzun, C.; Casanova, D.; Alemany, P.; Avnir, D.; Kizner, Z.; Sterkin, A. *J. Comput. Chem.* **2008**, *29*, 2712. (d) Pinsky, M.; Casanova, D.; Alemany, P.; Alvarez, S.; Avnir, D.; Dryzun, C.; Kizner, Z.; Sterkin, A. *J. Comput. Chem.* **2008**, *29*, 190. (e) Alvarez, S.; Alemany, P.; Avnir, D. *Chem. Soc. Rev.* **2005**, *34*, 313.

(2) Dryzun, C.; Avnir, D. *Phys. Chem. Chem. Phys.* **2009**, *11*, 9653.

(3) Casanova, D.; Falceto, A.; Alemany, P.; Carreras, A.; Alvarez, S. *J. Comput. Chem.* **2013**, *34*, 1321.

(4) (a) Casanova, D.; Alemany, P. *Phys. Chem. Chem. Phys.* **2010**, *12*, 15523. (b) Alemany, P.; Casanova, D.; Alvarez, S. *Phys. Chem. Chem. Phys.* **2012**, *14*, 11816.

(5) Ceulemans, A.; Beyens, D.; Vanquickenborne, L. G. *J. Am. Chem. Soc.* **1984**, *106*, 5824.

(6) Cirera, J.; Alemany, P.; Alvarez, S. *Chem.—Eur. J.* **2004**, *10*, 190.

(7) Cirera, J.; Ruiz, E.; Alvarez, S. *Chem.—Eur. J.* **2006**, *12*, 3162.

(8) Cirera, J.; Ruiz, E.; Alvarez, S. *Inorg. Chem.* **2008**, *47*, 2871.

(9) Cirera, J.; Alvarez, S. *Angew. Chem., Int. Ed.* **2006**, *45*, 3012.

(10) (a) Laporte, O.; Meggers, W. F. *J. Opt. Soc. Am.* **1925**, *11*, 459. (b) Gerloch, M.; Constable, E. C. *Transition Metal Chemistry*; VCH: Weinheim, Germany, 1994.

(11) Casanova, D.; Alemany, P.; Falceto, A.; Carreras, A.; Alvarez, S. *J. Comput. Chem.* **2013**, *34*, 1321.

(12) Turro, N. J.; Ramamurthy, V.; Scaiano, J. C. *Principles of Molecular Photochemistry: An Introduction*; University Science Books: Sausalito, CA, 2009.

(13) Kettle, S. F. A. *Physical Inorganic Chemistry: A Coordination Chemistry Approach*; Spektrum: Oxford, U.K., 1996.

(14) (a) Keinan, S.; Avnir, D. *J. Chem. Soc., Dalton Trans.* **2001**, 941. (b) Keinan, S.; Avnir, D. *Inorg. Chem.* **2001**, *40*, 318.

(15) Solomon, E. I. *Comments Inorg. Chem.* **1984**, *3*, 227.

(16) Ruiz-Martínez, A.; Casanova, D.; Alvarez, S. *Chem.—Eur. J.* **2010**, *16*, 6567.

(17) Casanova, D.; Cirera, J.; Llunell, M.; Alemany, P.; Avnir, D.; Alvarez, S. *J. Am. Chem. Soc.* **2004**, *126*, 1755.

(18) Llunell, M.; Casanova, D.; Cirera, J.; Alemany, P.; Alvarez, S. *SHAPE (version 2.0)*; Universitat de Barcelona: Barcelona, Spain, 2010, http://www.ee.ub.es.

(19) Alvarez, S.; Avnir, D. *Dalton Trans.* **2003**, 562.

(20) Becke, A. D. *J. Chem. Phys.* **1993**, *98*, 5648. Stephens, P. J.; Devlin, F. J.; Chabalowski, C. F. *J. Phys. Chem.* **1994**, *98*, 11623.

(21) Weigend, F.; Ahlrichs, R. *Phys. Chem. Chem. Phys.* **2005**, *7*, 3297.

(22) Shao, Y.; et al. *Phys. Chem. Chem. Phys.* **2006**, *8*, 3172.